Global Optimization of a Horizontal Axis Tidal Current Turbine with Shroud

Daisaku Sakaguchi [#1], Yusaku Kyozuka [#2]

[#1]*Graduate School of Engineering, Nagasaki University*

[#2]*Organization for Marine Sci. & Tech., Nagasaki University*
1-14 Bunkyo-machi, Nagasaki 852-8521, Japan

[1]daisaku@nagasaki-u.ac.jp

[2]kyozuka@nagasaki-u.ac.jp

Abstract— **A global search optimization system is applied for design of a horizontal axis tidal current turbine with shroud. 11 design parameters of the turbine blade and 4 design parameters of the shroud casing are considered for the optimization search by a genetic algorithm. For reducing the simulation cost, a neural network is applied as the meta-model of the RANS solver. Multi-objectives of a power coefficient at different tip speed ratio are applied for giving a function of wide operating range of the turbine. A proposed optimized design of the turbine shows a high output shaft power under a low tip speed ratio. Internal flow of the optimized horizontal axis tidal current turbine is discussed in detail. It is found that the optimized blade generates swirling flow and suppress flow separation at the diffuser wall. The wide angle of the diffuser successfully achieves higher pressure recovery ratio and results in a high suction power at the inlet of the turbine. It is found that the high performance tidal turbine is possible to design if both the blade and the shroud diffuser are optimized in same time.**

Keywords— **Multi-Objective Optimization, Genetic Algorithms, Artificial Neural Network, Tidal Current**

I. INTRODUCTION

Ocean energy has a high potential as renewable energy resource. However, issues of renewable energy are based on its unstableness. At the point of view of the stability of the energy, tidal current energy is one of the candidate [1] which is produced by an attraction of the moon and the sun. The frequency of the tidal flow is almost constant, and the maximum speed of the flow can be estimated without weather climate. Recently, various-shaped current turbines [2-4] are proposed, a perpendicular axis turbine such as a Darius turbine [5], which has an advantage in maintenance cost because its generator is possible to design to be located above the water surface. An axial type turbine is suitable for higher velocity conditions, and a higher efficiency is achieved based on the lift effect.

A high efficiency shrouded wind turbine is proposed by Oya [6] as is called the wind lens turbine. A brim at the end of the diffuser generate a wake region, and it works as an artificial wall. As results, higher pressure recovery obtained instead of a short axial length of the diffuser, and it promise a higher incoming flow based on a suction effect of the diffuser. Internal flow of the wind lens turbine has numerically analyzed by Furukawa [7], and optimization design method has been applied.

In this research, wind lens technology is applied for a horizontal axis tidal current turbine as is called Water Lens Turbine [8]. A global search of an optimization system [9] is applied for design of the turbine and shroud casing. 11 design parameters of the turbine blade and 4 design parameters of the shroud casing are considered for the optimization search by a genetic algorithm. For reducing the simulation cost, a neural network is applied as the meta-model of the RANS solver in this case. Multi-objectives of a power coefficient at different tip speed ratio are applied for a function of a wide operating range of the tip speed of the turbine. The final goal of this study is to propose an optimized shape of turbine with wide operating range and understand the flow physics of the diffuser effect.

II. NUMERICAL ANALYSIS AND OPTIMIZATION METHOD

A. Target turbine and numerical approach

The target turbine generator as shown in Fig.1 is 7 kW with a blade diameter of D_1= 1,000 mm. The turbine has 3 blade and a baseline thickness based on NACA4616 aero-foil. The diffuser has a function of a floating body and there is no limitation of the body weight for the tidal current turbine. Though the interesting physics of the wind lens technology is brim effect, it is not applied for the water lens turbine in this study. As shown in Fig.2, for the numerical simulation, an inlet boundary is set two times of D_1 far from turbine inlet, an outlet boundary is three times of D_1, and an external region is four times larger than D_1. For the tidal turbine, an artificial diffuser wall with zero thickness is applied for instance generating a numerical mesh. It is effective to generate a good quality of the computational mesh by unstructured mesh for the external flow and structured mesh for the internal flow of the shrouded turbine.

In this study, 130 thousand nodes of unstructured mesh in stationary domain is generated by ANSYS ICEM-CFD, and

450 thousand nodes of structured mesh in rotational domain is generated by ANSYS Turbogrid. Each domain is connected by domain interface of Frozen Rotor Interface. The working fluid is water and the axial component of velocity at the inlet boundary is kept constant speed of U_0=1.0 me/s. The rotational speed of the turbine has changed for varying a tip speed ratio λ_0 as defined in Eq. (1). The output shaft power is normalized as a power coefficient C_{p0} by using a reference are of A_1 at blade inlet as shown in Eq. (2). The power coefficient C_{p0} is defined for the turbine without shroud and it has a meaning of the efficiency of the turbine. However, in the case of the current study of the shrouded turbine, the accelerated flow at the turbine inlet U_1 is different from U_0. It is reminded here that the power coefficient C_{p0} does not have a meaning of efficiency of turbines in the case of the shrouded turbine. The reason of why the power coefficient C_{p0} is applied in this study is that it is useful parameter when estimate the output power from the different diameter of the blade and flow condition of the tidal flow. The efficiency of the shrouded turbine is discussed at the latter section in this paper.

$$\lambda_0 = \frac{D_1 \cdot \omega}{2 \cdot U_0} \tag{1}$$

$$C_{p0} = \frac{Trq \cdot \omega}{0.5 \cdot \rho \cdot A_1 \cdot U_0^3} \tag{2}$$

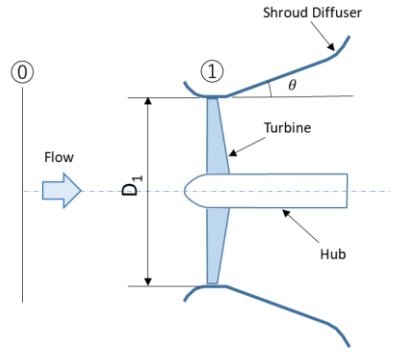

Fig. 1 Meridional section of a horizontal axis tidal current turbine with shroud

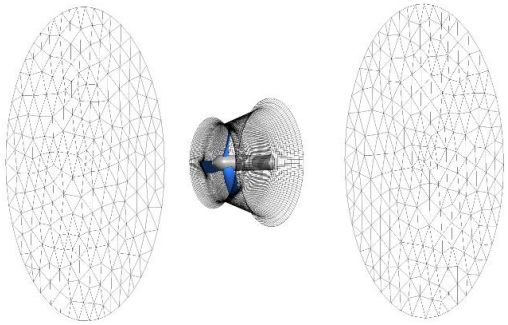

Fig. 2 Computational mesh with a structured mesh for internal of the turbine flow and an unstructured mesh for outer flow of the turbine

B. Optimization system

An optimization system used in the current research was developed by von Karman Institute for Fluid Dynamics and it is applied to variety of turbomachinery applications. The general idea of the optimization system is described as shown in Fig.3. The vertical flow from top to down on the left figure represents the traditional design procedure in which theoretical consideration and experimental experience play a crucial role. The upper right box (Level 1) represents the optimization loop comprising of a differential evolution algorithm (DE) and a meta-model based on an Artificial Neural Network (ANN). The ANN replaces the computationally expensive CFD simulations in the optimization loop (Level 1) and provides less accurate but very fast performance predictions to evaluate the larger number of geometries by the differential evolution algorithm during its search for the optimum. For training the meta-model for prediction, a database is required from a past experienced reliable numerical data. The database is, therefore, initialized by means of a Design of Experiment (DOE) comprising 64 designs in an advance optimization loop (Level 1) starts. After building a database and training the meta-model (ANN), the optimization loop (Level 1) is invoked and DE predicts the optimal geometries. However, ANN requires a validation which is then performed in the feedback loop (Level 2). The optimal geometries coming from the ANN prediction are confirmed by the more computationally accurate and expensive CFD calculations to verify the accuracy of the meta-model (Level 2). The results of the accurate performance analysis are added to the database and a new optimization loop is started after a new training of the meta-model on the enlarged database.

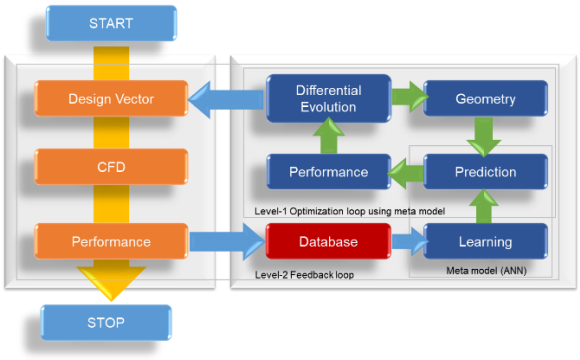

Fig. 3 General layout of the VKI optimization system

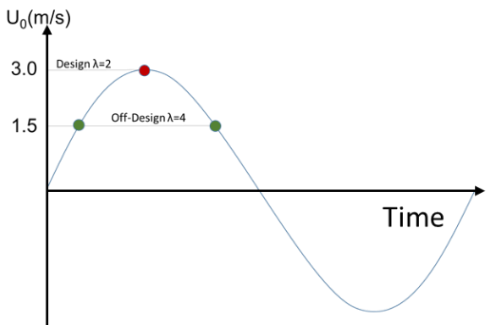

Fig. 4 Sinusoidal motion of the current velocity of tidal flow

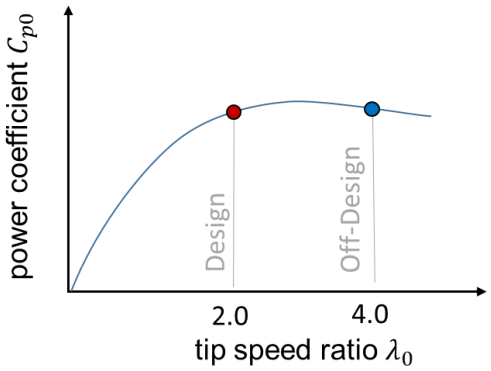

Fig. 5 Objective function of power coefficient with different tip speed ratio

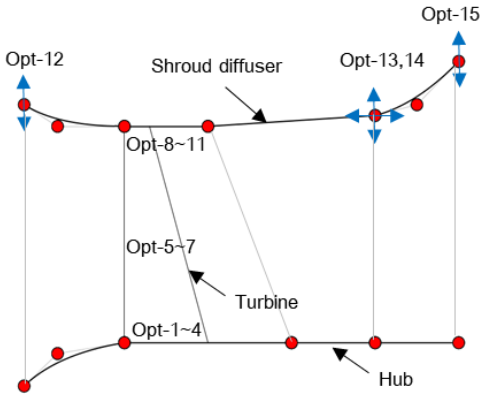

Fig. 6 Control points of design variable for optimization

C. *Objective function and design parameters*

As an ideal speed of the tidal flow changes in a sinusoidal motion with a period of almost every 6 hours as shown in Fig.4. The maximum speed of tidal current at experimental site at GOTO island in Japan [10] is 3.0 m/s which corresponds to the design tip speed ratio of λ_0 = 2.0, and medium speed of tidal current is 1.5 m/s which corresponds to the off-design tip speed ratio of λ_0 = 4.0. As shown in Fig.5, the objectives for the optimization search in this study is maximize the power coefficient at design and off-design tip speed ratio. It means that optimized turbine design is searched which maximize an output power under different tidal current speeds.

The upper and lower limit of design parameters for the optimization are shown in Table 1. A blade angle and a chord length of the turbine blade has changed at hub and shroud, a point of inflection is introduced to have a three-dimensional shape of the turbine. As shown in Fig.6, 3 control points (opt-12, 13, 14) for the shroud casing are adopted for changing the conical diffuser length and diameter. Additional parameter of the opt-15 is for smooth extension of the diffuser exit.

TABLE 1 DESIGN PARAMETERS FOR OPTIMIZATION OF WATER LENS TURBINE

Param #	Blade Hub	Min	Max
Param-1	AxialPump.Geo.Blade.Hub.Beta.Point1.Y	5	15
Param-2	Delta_HubBeta_12	5	15
Param-3	Delta_HubBeta_23	0	10
Param-4	AxialPump.Geo.Blade.Hub.Meridional.Point2.X	0.08	0.12
	Blade Mid1	Min	Max
Param-5	AxialPump.Geo.Blade.Mid1.Level	0.1	0.5
Param-6	AxialPump.Geo.Blade.Mid1.DeltaTheta.Point1.Y	0	5
Param-7	AxialPump.Geo.Blade.Mid1.DeltaTheta.Point2.Y	-20	0
	Blade Shroud	Min	Max
Param-8	AxialPump.Geo.Blade.Shr.Beta.Point1.Y	55	62
Param-9	Delta_ShroudBeta_12	0	15
Param-10	Delta_ShroudBeta_23	0	5
Param-11	AxialPump.Geo.Blade.Shr.Meridional.Point2.X	0.03	0.05
	Shroud Casing	Min	Max
Param-12	AxialPump.Geo.Meridional.Patch1.Shr.Point1.Y	0.5	0.58
Param-13	AxialPump.Geo.Meridional.Patch3.Shr.Point2.X	0.3	0.64
Param-14	AxialPump.Geo.Meridional.Patch3.Shr.Point2.Y	0.5	0.7
Param-15	Delta_ShroudOuterRadius	0	0.12

III. RESULTS AND DISCUSSION

The optimization result is shown in Fig.7 as a two correlation of the two objectives space. The horizontal axis shows the power coefficient C_{p0} at the design tip speed ratio of λ_0=2.0, and the vertical axis shows the power coefficient at off-design tip speed ratio of λ_0=4.0. In this study, the optimizer try to solve the problem as minimize, so each objective is multiplied by -1, and the lower left corner of the figure shows good candidate. The black circles indicate the individuals by the DOE process for the initial learning of the ANN. The red circles indicate the individuals from searching system GA+ANN. Totally 150 individuals are considered during the optimization process of the Level-2 loop as shown in Fig.3. A hyperbolic shape of the front end of the individuals forms a Parato front, which indicates that two objective functions are under a trade-off condition and it is difficult to improve both objective functions in same configuration of the turbine.

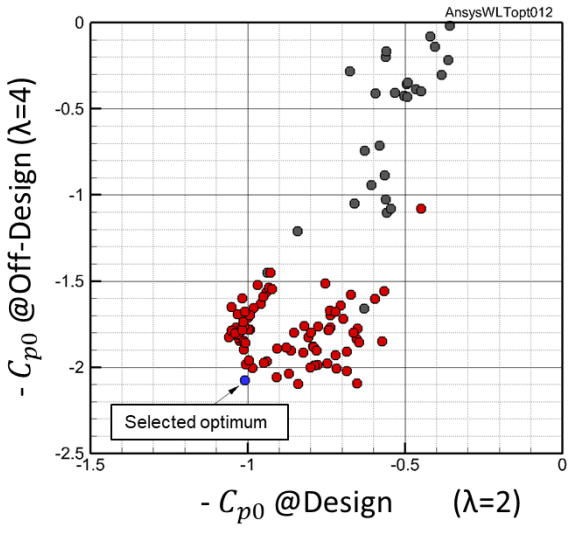

Fig. 7 Optimization result on two objective space

One of the individual of the red circle is selected as an optimum which is indicated by a blue circle in Fig.7. The selected optimum shows good balance for both of objectives.

A three-dimensional shape of the selected optimum is shown in Fig.8. All of design parameters are listed in Table.2. The outlet diameter of the diffuser is 1.64 D_1, which is the maximum size of the diffuser within the range of the design parameter. The turbine blade shows the three-dimensional skewed shape. A stagger angle is 19.5 deg. at hub side, and it is 73.5 deg. at shroud side.

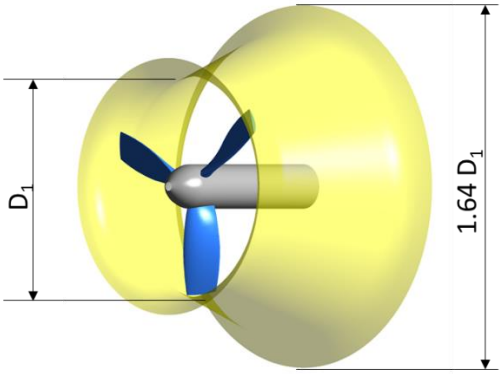

Fig. 8 Optimized blade and shroud

TABLE 2 OPTIMIZED DESIGN PARAMTERS

Param #	Blade Hub	Optimized
Param-1	AxialPump.Geo.Blade.Hub.Beta.Point1.Y	15
Param-2	Delta_HubBeta_12	12.4
Param-3	Delta_HubBeta_23	1.1
Param-4	AxialPump.Geo.Blade.Hub.Meridional.Point2.X	0.12
	Blade Mid1	Optimized
Param-5	AxialPump.Geo.Blade.Mid1.Level	0.5
Param-6	AxialPump.Geo.Blade.Mid1.DeltaTheta.Point1.Y	5
Param-7	AxialPump.Geo.Blade.Mid1.DeltaTheta.Point2.Y	-6.6
	Blade Shroud	Optimized
Param-8	AxialPump.Geo.Blade.Shr.Beta.Point1.Y	55
Param-9	Delta_ShroudBeta_12	15
Param-10	Delta_ShroudBeta_23	5
Param-11	AxialPump.Geo.Blade.Shr.Meridional.Point2.X	0.05
	Shroud Casing	Optimized
Param-12	AxialPump.Geo.Meridional.Patch1.Shr.Point1.Y	0.58
Param-13	AxialPump.Geo.Meridional.Patch3.Shr.Point2.X	0.64
Param-14	AxialPump.Geo.Meridional.Patch3.Shr.Point2.Y	0.69
Param-15	Delta_ShroudOuterRadius	0.12

Velocity vector and contour plot on the meridional plane are shown in Fig.9 and 10. The optimized diffuser shows smooth flow along the diffuser wall without flow separation. The shrouded diffuser expands its diameter to the downstream, and if the flow diffused to the downstream, flow velocity will be decelerated. The decelerated flow gives a positive static pressure gradient from inlet to the outlet of the diffuser. If the good velocity deceleration achieved, higher pressure gradient occurs, and it results in the higher incoming flow at the turbine inlet as shown in Fig.10, which is based on a negative static pressure gradient from suction inlet to the rotating turbine.

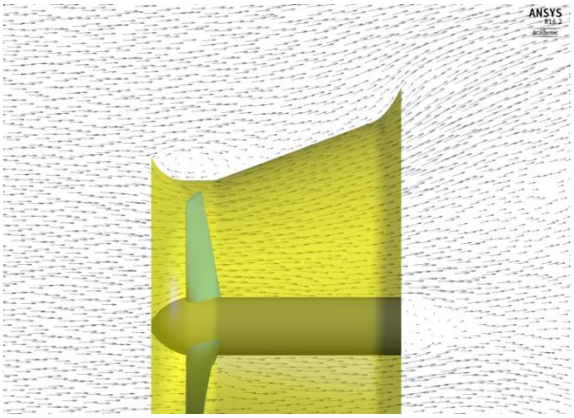

Fig. 9 Velocity vector on the meridional plane (λ_0=2.0)

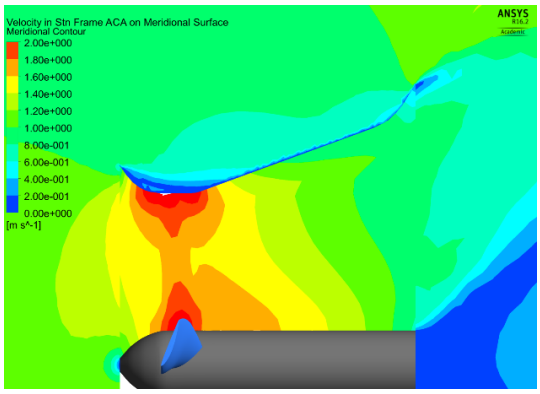

Fig. 10 Contour of circumferential averaged absolute velocity (λ_0=2.0)

A characteristics curve of the power coefficient C_{p0} is investigated by changing the tip speed ratio λ_0 as shown in Fig.11. Open circle shows in the case of the optimized turbine, the maximum power coefficient C_{p0} reaches to 2.0 at the off-design tip speed ratio λ_0= 4.0, and at the design tip speed of λ_0= 2.0, the power coefficient shows also high value of 1.0 comparing to the conventional axial turbine. As the reference, the case without shroud wall is shown as solid circle. The maximum power coefficient is around 0.2 and a working range of the tip speed ratio is less than 3.0. It is found that optimized turbine shows high power coefficient in wide operating tip speed range.

The effect of the shroud casing wall is seen from the investigation of the inlet velocity condition. Figure 12 shows change in the inlet velocity U_1 at the turbine inlet as a function of the tip speed ratio. As the tip speed ratio increases, the inlet velocity increases. At the reference points of the off-design condition of λ_0= 4.0, almost 2 times of the velocity is obtained by the effect of the diffuser. An interesting point is very high velocity of U_1/U_0=1.85 is achieved at the design condition of λ_0= 2.0. It is understood that the higher power coefficient in wider tip speed ratio as shown in Fig.11 is supported by the higher incoming flow at blade inlet.

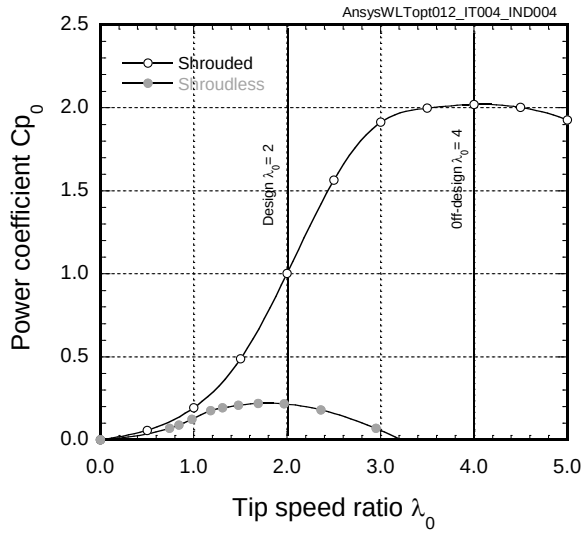

Fig. 11 Comparison of power coefficient curve between the case with the shrouded turbine and the shroud-less turbine

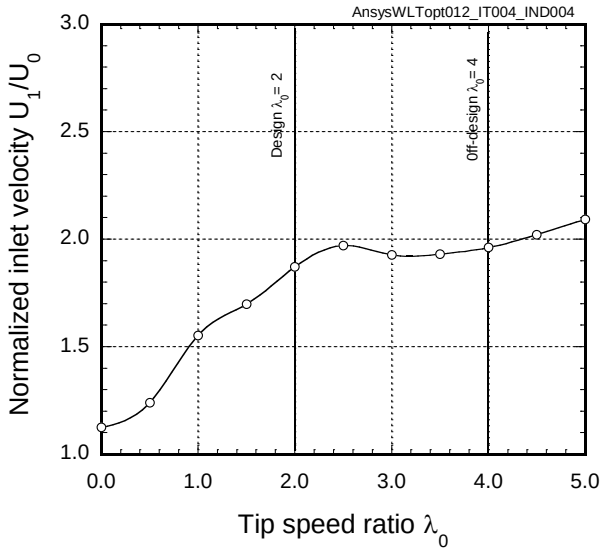

Fig. 12 Increment of inlet velocity based on the suction power of the shroud casing

In the optimization process, many individuals are simulated, and both of their design parameters and characteristics are stored at the Database as shown in Fig.3. All of individuals in the Database are analysed to make clear which design parameter is sensitive for the power coefficient.

Figure 13-(a) and (b) show a relationship between the power coefficient C_{p0} and a diffuser angle θ. During the optimization process, it is possible to search the diffuser angle from 0 to 35 degree. However, the optimizer try to find the best power coefficient at 21 degree. It is understood that if the diffuser angle is too small, deceleration of the velocity becomes small and results in the lower speed of the incoming flow at the blade inlet. If the diffuser angle is too large, flow will be separated at the diffuser wall and it is not expected the pressure recovery at the diffuser. It is found that the optimized diffuser angle is 21 degree in the present study.

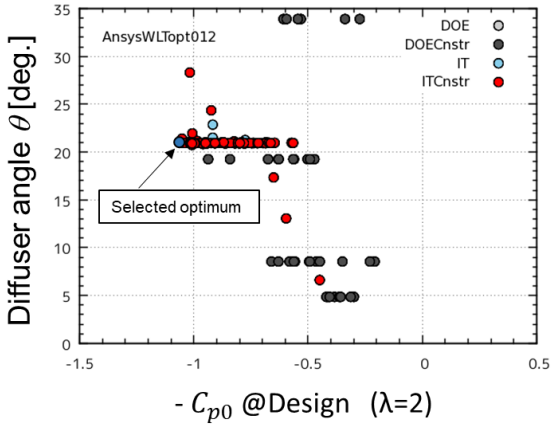

(a) Design condition (λ_0=2.0)

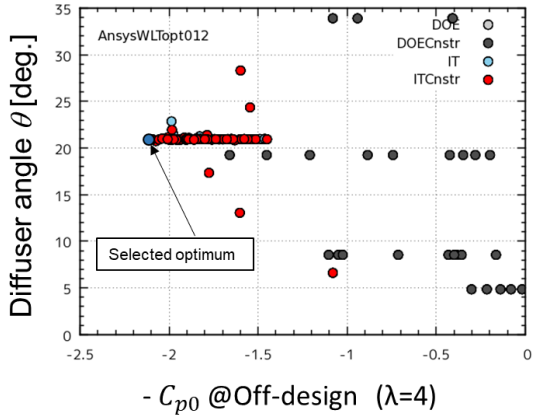

(b) Off-Design condition (λ_0=4.0)

Fig. 13 Relationship between power coefficient Cp_0 and diffuser angle θ

The main reason of why the optimum turbine shows good output of the power is considered by wider diffuser angle of 21 degree, which is larger than a conventional conical diffuser angle of 7~12 degree. [11] The question is why the diffuser works without flow separation. In Fig.14, contour of a circumferential component of absolute velocity is plotted. The velocity is circumferentially averaged and it is plotted on the meridional plane. A positive circumferential component of velocity is seen at the shroud side in the case of the design tip speed ratio of λ_0= 2.0. On contrary, in the case of the off-design tip speed ratio of λ_0= 4.0, the positive circumferential component of velocity is not large. The positive circumferential velocity is based on a separated flow from the rotating turbine at shroud tip as shown in Fig.15. Three dimensional ISO surface of the circumferential component of velocity is spread to downstream from the shroud tip in the case of the design tip speed ratio of λ_0= 2.0. Figure 16 shows the contour plot of the circumferential component of velocity at several axial position inside of the diffuser. In the case of the design tip speed ratio of

λ_0= 2.0, positive circumferential velocity has same tip speed of the blade tip, and it spread to the downstream. The flow with circumferential component of velocity spreads to downstream along the shroud wall based on the centrifugal force, and the centrifugal force suppress the flow separation at the diffuser. It is clear the centrifugal force based on the tangential velocity at shroud tip suppresses flow separation at diffuser, if the diffuser works without flow separation, static pressure at turbine inlet will reduce, and as results incoming flow to the blade inlet increases by the pressure difference. Increased incoming flow to the turbine blade improves the output torque of the turbine. The physical motion of the tip flow with high swirl flow suppress the flow separation of the diffuser is unique. The phenomena occurs especially in the case of the design tip speed ratio of λ_0= 2.0. In the case of the off-design tip speed ratio of λ_0= 4.0, blade stagger angle is adjusted to the flow and a large amount of a suction power is expected by high blade loading of the turbine. It is impossible to adjust the stagger angle for two different tip speed conditions, the optimized shape of the turbine try to over-loads the flow at the shroud tip under low tip speed conditions. Though the flow separation occurs and blade loading is very small, swirl flow at the diffuser increases the suction power of the diffuser and results in the higher incoming velocity at blade inlet as shown in Fig.12.

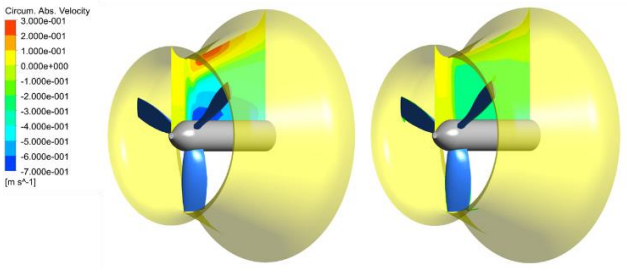

(a) λ_0=2.0 (b) λ_0=4.0

Fig. 14 Contour of averaged circumferential component of absolute velocity

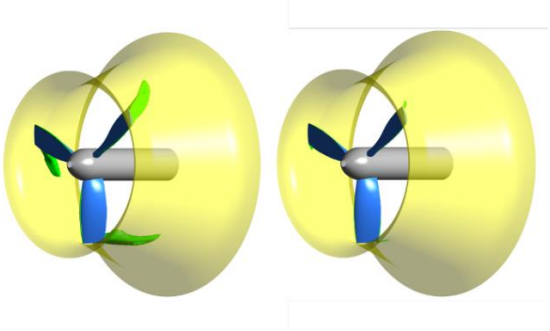

(b) λ_0=2.0 (b) λ_0=4.0

Fig. 15 ISO-surface of circumferential component of absolute velocity 2.0 m/s

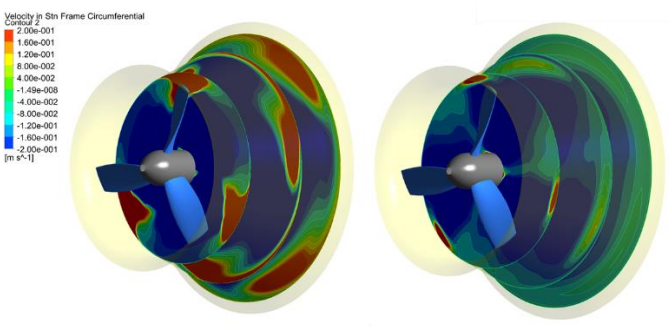

(c) λ_0=2.0 (b) λ_0=4.0

Fig. 16 Contour of circumferential absolute velocity in 3 axial positions

It is important to understand the point view of the efficiency. In this paper, two efficiencies for the turbine and diffuser are proposed as following equations. The output shat power is normalized by a total kinetic energy and volume flow rate at blade inlet. The representative velocity is taken by the velocity at blade inlet U_1 and a shaft power coefficient is defined as following,

$$C_{p\_shaft} = \frac{Trq \cdot \omega}{0.5 \cdot \rho \cdot U_1^2 \cdot A_1 \cdot U_1} \quad (3)$$

A diffuser power coefficient is defined as a static pressure recovery normalized by a dynamic pressure at blade inlet.

$$C_{p\_diffuser} = \frac{(p_0 - p_1)}{0.5 \cdot \rho \cdot U_1^2} \quad (4)$$

Finally, a total power coefficient of the Water Lens Turbine (WLT) is defined as the combination of eq.(3) and (4),

$$C_{p\_WLT} = C_{p\_shaft} + C_{p\_diffuser} \quad (5)$$

The proposed power coefficient of WLT is the total efficiency for the shrouded axial turbine which has a meaning of how much energy is converted to the output shaft and the pressure recovery of the diffuser.

Figure 17 shows change in power coefficients as defined in Eq. (3), (4) and (5). The interesting function of the optimized WLT is the diffuser power coefficient $C_{p\_diffuser}$ is very high in whole tip speed ratio. Thanks to the high performance of the diffuser, incoming flow velocity at inlet of the blade is very high even though the tip speed ratio is low as shown in Fig.12. Under the low tip speed conditions, the flow angle does not match to the stagger angle of the blade, however the diffuser works well and increased incoming flow support the high output shaft power.

It is found that the improvement of the power coefficient is achieved by the synergy effect between the diffuser and the turbine blade, and it is possible to design by optimization search taking into consideration of the design parameters of diffuser and turbine blade.

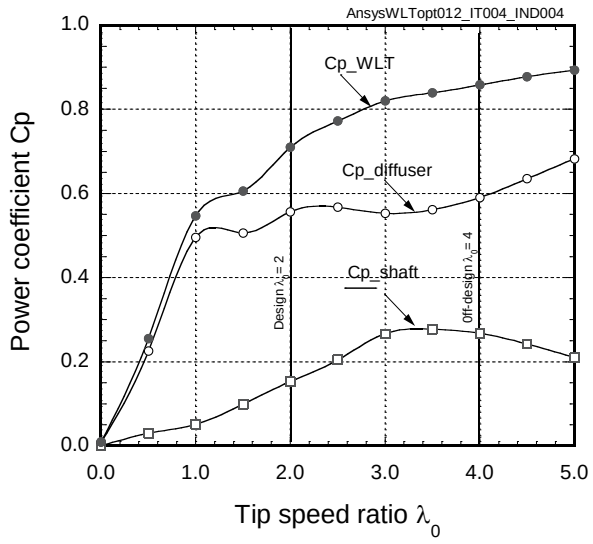

Fig. 17 Change in power coefficients as function of the tip speed ratio

IV. Conclusions

The multi-objective optimization was studied for design of the water lens turbine. 11 design parameters of the turbine blade and 4 design parameters of the shroud casing were considered for the optimization search by a genetic algorithm. For reducing the simulation cost, a neural network was applied as the meta-model of the RANS solver in this case. Multi-objectives of a power coefficient at different tip speed ratio were applied for a function of a wide operating range of the turbine. It is found that the optimized horizontal axis tidal current turbine is possible to design by the meta-model assisted optimization system. It is clearly shown that swirl flow at the shroud side of the turbine exit suppresses the flow separation at diffuser based on the centrifugal force. The effect of the swirl flow works under low tip speed conditions and proposed power coefficient shows clear effect of the diffuser.

References

[1] Yamada, H., Nakata, K., Evaluation of Ocean Energy Potential in Japan, Journal of Advanced Marine Science and Technolgy, Vol.19, No.1, 43-47, 2013

[2] Shiono, M., Suzuki, K. and Kiho, S., An Experimental Study of the Characteristics of a Darrieus Turbine for Tidal Power Generation, Electrical Engineering in Japan, Vol. 132, No. 3, 2000.

[3] Keysan, A. S. McDonald, M. Mueller, A Direct Drive Permanent Magnet Generator Design for a Tidal Current Turbine(SeaGen), Electric Machines & Drives Conference (IEMDC), 2011 IEEE International, 224-229, 2011

[4] http://www.openhydro.com/

[5] M. Shahsavarifard, E. L. Bibeau, V. Chatoorgoon Effect of shroud on the performance of horizontal axis hydrokinetic turbines,Ocean Engineering Volume 96, 1 March 2015, Pages 215-225

[6] Y. Ohya, T. Karasudani, A Shrouded Wind Turbine Generating High Output Power with Wind-lens Technology, Energies, 3, 634-639, 2010

[7] N. Oka, M. Furukawa, K. Kawamitsu and K. Yamada, Optimum aerodynamic design for wind-lens turbine, Journal of Fluid Science and Technology, Vol. 11, No. 2 p. JFST0011, 2016

[8] H. Sun, Y. Kyozuka, Experimental Validation and Numerical Simulation Evaluation of a Shrouded Tidal Current Turbine, Journal of the Japan Society of Naval Architects and Ocean Engineers, Vol. 16, 25-32, 2012

[9] D. Sakaguchi, M. Ishida, H. Hayami, L. Mueller, Z. Alsalihi and T. Verstraete, Multipoint Multi-objective Optimization of a Low Solidity Circular Cascade Diffuser in Centrifugal Blowers, Proceedings of ASME Turbo Expo 2014: Turbine Technical Conference and Exposition, GT2014-26013,pp.1-10, (2014)

[10] H. Sun, S. Yamaguchi and Y. Kyozuka, Tidal Current Energy Assessment Around Goto Islands, Japan, Proceeding of the International Symposium on Marine and Offshore Renewable Energy (MORE), 1-8, 2013

[11] McDonald, A.T. and Fox, R.W., Incompressible. Flow in Conical Diffusers, ASME 65-FE-25, 1965